MULTIPHASE FLOW PERFORMANCE IN PIPING SYSTEMS

Mahmoud Elsharafi, Christopher J. Alexis, and Trevon Antoine
McCoy School of Engineering, Midwestern State University

ABSTRACT
Multiphase flow is found in nature and in different industries, however, it is prevalent in the petroleum production industry. This phenomenon gives rise to the major issue of pressure loss within piping systems that ultimately decreases production. Multiphase flow has been studied for decades, but there is now a greater need for its study with the increase in unconventional engineering methods. This study investigates various phenomena related to multiphase flow, such as flow regimes, pressure loss produced by friction, pipe orientation, and different fluid phase properties. An experimental system was designed in which different fluid phases were used to represent varying situations in piping systems. The system included horizontal, inclined, and vertical pipe orientations as experienced during hydrocarbon migration from the reservoir to the surface. To replicate industry multiphase flow in the experimental system, water was used to represent the oil and compressed air to represent gas. The pressure differences throughout the system were calculated using the Beggs and Brill Correlation and the Lockhart-Martinelli Parameter along with the Chisholm Equation. Experimental pressure differences and the effect of the choke valve positions were also recorded for the different sections of the system while observing the flow regimes produced by multiphase interaction. The research methods found that most of the hydrostatic pressure losses occurred in the elbows, and most frictional pressure losses occurred in the vertical 3ft pipe. In contrast, the 45° and 90° downhill pipes experienced increased pressure which suggests that pipe orientation had the most influence on the pressure.

INTRODUCTION

The term multiphase flow or two-phase flow refers to the simultaneous flow of more than one fluid phase through a porous medium (Sun, 2016). There are three natural phases of materials, namely solid, liquid, and vapor or gas (Michaelides et al., 2016). Hence, multiphase flow is found in various places both in nature and in practice. However, multiphase flow is prevalent in the petroleum production industry, where its comprehension is very important since it can offer significant economic savings (Bai et al., 2012). In nature, multiphase flow is found in various natural phenomena such as different forms of precipitation, namely rain and snow, and sediment transportation such as avalanches and landslides. In industry, multiphase flow occurs in oil and gas wells, gathering systems, and many other piping systems where fluids are transported from one location to another. The effective transportation of liquids is vital to human productivity, where pipes of a circular cross-sectional area are most frequently used in piping systems due to its structural advantage compared to any other shape. Specifically, circular pipes are used in the subsurface and at the surface in the oil and gas industry. Circular pipes can withstand varying pressure differences between internal and external pressures without worrying about deformation. This structural advantage is significant in the subsurface, where both internal and external pressures are generally higher than pressures experienced at the surface (Okoye, 2016).

During production, crude oil is usually a mixture of gas, oil, and water or brine, which means multiphase flow to the surface is generally unavoidable (Sun, 2016). The simultaneous migration of multiple fluid phases in the wellbore produces a major issue in the petroleum industry characterized as pressure loss. The pressure is an essential component during petroleum production as it determines the quantity and rate of hydrocarbons that can be retrieved from the subsurface to be later refined at the surface and subsequently used as energy and other petroleum products. The importance of pressure is related to three important petroleum production phases over a well's lifespan known as primary, secondary, and tertiary or enhanced oil recovery. These three phases are defined by the percentage of original oil in place retrieved or recovered from the reservoir and their corresponding methods of oil recovery. Primary oil recovery retrieves approximately 5% - 15% of the well's potential with the use of the natural reservoir pressure for oil migration, while secondary oil recovery can retrieve an additional 30% with the use of fluid injection

(typically water) to increase the pressure and displace the oil as natural reservoir pressures decrease. The final phase, tertiary or enhanced oil recovery is a more aggressive and costly recovery method used to produce an additional 30% - 60% of the hydrocarbons after primary and secondary recovery pressures decrease. This recovery method uses various techniques such as CO2 injection, natural gas miscible injection, and steam recovery (Alagorni et al., 2015).

The recovery and production of petroleum can be further separated into two broad categories of conventional and unconventional engineering processes. Conventional oil reservoirs use traditional drilling and pumping methods, while unconventional oil cannot be recovered using conventional or traditional drilling and pumping methods. With decades of experience in conventional wells, there are well-established methods to combat multiphase flow fluid problems in those wells. However, the increase in unconventional wells and the decrease in conventional oil production relative to unconventional production give rise to new issues relating to multiphase flow such as underbalanced drilling, well control for kicking, acidic gas wells, and the well control for deep-water drilling making theoretical multiphase flow studies increasingly important in the 21st century (Sun, 2016).

The interaction of multiple fluid phases produces different fluid flow patterns known as flow regimes. These regimes are operating conditions, fluid properties, flow rates, pipe orientation, and geometry (Corneliussen et al., 2005). Imagining the behavior of multiphase flow in an untested system without imagining how the phases are arranged given different parameters can be very difficult. Flow regime maps are used to predict different flow patterns by correlating the parameters such as their velocity (Griffith, 1984). However, the determination of flow regimes in operating piping systems is generally difficult, which necessitates laboratory experiments to understand flow regimes better. In the laboratory, multiphase flow regimes can be studied through transparent piping by direct visual observation and subsequent characterization. The functions of flow regimes created by multiphase flow produce more concepts that clarify the factors that influence pressure differences within piping systems. As multiphase flow occurs through a pipe, the pipe's volume occupied by a single-phase is often different from its proportion of the total volumetric flow rate due to the density differences between the different phases occupied by the pipe. In an upward flow, being inclined or vertical, the density difference between fluid phases causes the dense phase to "slip down" or be "held up" since the lighter phase is moving faster through the pipe than the denser phase. As a result, the in-situ volume fraction of the denser phase will be greater than input volume fraction. This also means the in-situ volume fraction of the lighter will be less than its input volume fraction phase (Sarah et al., 2014). This concept is known as liquid "holdup," where its value can be quantitatively determined using correlation methods produced by previous experimental research.

Due to the complexity of multiphase flow, accurately predicting pressure loss in piping systems has proven difficult. This problem has given rise to many specialized solutions for limited multiphase flow conditions without any single solution accepted for broad operating conditions. This again creates a great need for the study of multiphase flow. In addition, for any segment of the pipe, the liquid velocity along the pipe wall can vary over short distances without any major change in fluid property or pipe orientation. This result in variable frictional pressure loss due to liquid throughout any piping system with multiphase flow. During other conditions, which can be represented by flow regimes, the liquid phase can be almost completely entertained in the gas phase where the gas is represented by a film around the walls of the pipe and the liquid within the core of the multiphase. This result in the liquid phase having very little influence on frictional pressure loss for that specific situation (Orkiszewski, 1967).

Due to the complexity of multiphase flow, accurately predicting pressure loss in piping systems has proven difficult. This problem has given rise to many specialized solutions for limited multiphase flow conditions without any single solution accepted for broad operating conditions. This again creates a great need for the study of multiphase flow. In addition, for any segment of the pipe, the liquid velocity along the pipe wall can vary over short distances without any significant change in fluid property or pipe orientation. This results in variable frictional pressure loss due to liquid throughout any piping system with multiphase flow. During other conditions, which flow regimes can represent, the liquid phase can be almost completely entertained in the gas phase, where the gas is represented by a film around the pipe walls and the liquid within the core

of the multiphase. This results in the liquid phase having very little influence on frictional pressure loss for that specific situation (Orkiszewski, 1967).
Later, Hagedorn and Brown (1965) published an empirical two-phase flow correlation that doesn't distinguish between the flow regimes. However, they developed this correlation from 475 tests in a 1,500-foot experimental well using fluids with viscosities up to 110 centipoises and through 1 inch, 1¼ inch, and 1½ inch nominal size tubing. They found there is no change to holdup with deviation (Hagedorn and Brown, 1965). Following Hagedorn and Brown, Beggs and Brill (1973) developed a correlation by experimental study of a two-phase flow in horizontal and inclined pipes. They designed a system of 1 inch and 1 ½ inch smooth circular pipes to investigate the effect of inclination on liquid holdup and pressure loss in gas and liquid two-phase flow (Beggs and Brill, 1973). Then, Stuhmiller (1977) studied the influence of interfacial pressure forces on the character of two-phase flow model equations in 1977. In addition, Zhang and Prosperetti (1997) found that phase interactions also result in stress in a potential flow, while Taitel and Dukler (1980) introduced the description of the simultaneous flow of gas and liquid in vertical pipes, with names such as bubble, slug, and annular flow. Their results are shown in the form of a cross plot with the superficial gas velocity (vgs), on the x-axis and the superficial liquid velocity (vls), on the y-axis, which is shown in figure 2 (Taitel et al., 1980).

Today, there are numerous well-defined flow regimes such as bubble, slug, plug, churn, annular, stratified, stratified wavy and mist flows (figure 3). However, these flow regimes can be grouped into three main flow regime categories: segregated or separated flow, intermittent flow, and dispersed flow (Corneliussen et al., 2005). Corneliussen et al., (2005) described that segregated or separated flow is characterized by a non-continuous phase distribution in the radial direction and a continuous phase in the axial direction of the pipe where flows such as stratified and annular flow fall under this category. In addition, Corneliussen et al. (2005) described intermittent flow as being non-continuous in the axial direction, which therefore results in a locally unsteady behavior. Flows such as elongated bubble, churn, plug, and slug flow fall under intermittent flow. Corneliussen et al. (2005) further outlined dispersed flow as to where uniform phase distributions are both in the pipe's radial and axial directions where flows such as bubble and mist flow fall under this category, as shown in figure 3.

THEORY

In order to calculate pressure losses within our system, we had to find accurate methods. We evaluated various correlations, including research done by Lockhart-Martinelli (1949), Fancher and Brown (1963), Duns and Ros (1963), Hagedorn and Brown (1965), and Beggs and Brill (1973). After extensive evaluation and careful consideration, we decided the Lockhart-Martinelli (1949) and Beggs and Brill (1973) would yield the most accurate results given our system and parameters. The Beggs & Brill correlation is used to calculate the pressure drop in the vertical and inclined sections present in our system, which requires the knowledge of the different flow patterns present in the pipes as well as the liquid velocity number and Froude's number.

The Lockhart-Martinelli parameter is used to calculate the two-phase pressure drop in the horizontal sections of the system. The Lockhart-Martinelli (1949) parameter is defined as the square root of the pressure gradient ratio of liquid to the pressure gradient of gas or vapor. As such, the pressure gradient of both phases (liquid and air) has to be calculated separately (Kutty et al., 2017). After the pressure gradient is found for each phase, the Chisholm (1967) equations are used as multipliers to combine both pressure gradients, yielding the total pressure loss of the horizontal section of the piping system.

Horizontal Pipe Orientation (Lockhart-Martinelli Parameter & Chisholm Equation)

Pressure Gradient Calculations

For this research, one of the main concerns was determining pressure losses experienced throughout the experimental system. As mentioned before, the Lockhart-Martinelli method coupled with the Chisholm Equation was used to calculate the pressure losses in our horizontal sections. The following steps shown are used to ultimately find the total multiphase pressure gradient for horizontal sections in our experimental system.

In order to find the pressure gradient, the cross-sectional area, A_c is determined by the following formula

$$A_c = {D_H}^2 \quad (1)$$

The Mass Flux, j can then be calculated

$$j = \frac{\dot{m}}{A_c} \quad (2)$$

Once Mass Flux is calculated the Reynolds number, R_{H2O} is determined

$$R_{H2O} = \frac{j * D_H}{\mu} \quad (3)$$

Find friction factor, f_{H2O} is also calculated from Reynolds number

$${f_{H2O}}^{-0.5} = -1.8 log_{10}\left(\left(\frac{\frac{e}{D}}{3.7 D_H}^{1.11}\right) + \left(\frac{6.9}{R_{H2O}}\right)\right) \quad (4)$$

Lastly the pressure gradient, $(\Delta P/L)\ H_2O$ is calculated

$$\left(\frac{\Delta P}{L}\right)_{H2O} = \frac{f_{H2O} * (j_{H2O})^2}{2 * \rho_{H2O} * D_H} \quad (5)$$

The steps above are then repeated to find the pressure gradient for air using equations 1 – 5.

Lockhart-Martinelli Parameter

From the Pressure Gradient ($\frac{\Delta P}{L}$) the Lockhart-Martinelli parameter, X is given by:

$$X = \sqrt{\frac{\left(\frac{\Delta P}{L}\right)_{H2O}}{\left(\frac{\Delta P}{L}\right)_{air}}} \quad (6)$$

Total Multiphase Pressure Gradient

First the Water Pressure Gradient Multiplier (Chisholm Equation), φH_2O is given by:

$$\varphi_{\mathrm{H2O}} = (1 + 18X^{-1} + X^{-2})^{0.5} \quad (7)$$

Then, the Air Pressure Gradient Multiplier (Chisholm Equation) $\varphi_{air,}$ is also given by:

$$\varphi_{\mathrm{air}} = (1 + 18X^{-1} + X^{-2})^{0.5} \quad (8)$$

Finally the Multiphase Pressure Gradient, $(\Delta P/L)_{multi}$ can be found by the following equation:

$$\left(\frac{\Delta P}{L}\right)_{multi} = {\varphi_{\mathrm{H2O}}}^2 * \left(\frac{\Delta P}{L}\right)_{H2O} = {\varphi_{\mathrm{air}}}^2 * \left(\frac{\Delta P}{L}\right)_{air} \quad (9)$$

Moody Diagram

Using the Reynolds number from equation (3) and the Friction factor equation (4), the expected appropriate flow can be determined from the Moody diagram shown in figure 4. From the moody diagram and our calculations, we determined that flow would be turbulent based on our Reynolds Number being greater than 2300.

Vertical & Inclined Pipe Orientation (Beggs & Brill Correlation)

The Beggs and Brill (1973) correlation is one of the few published correlations capable of handling all the different flow directions. The correlation was developed by an experimental study of a two-phase flow in horizontal and inclined pipes. They designed a system of 1 inch and 1 ½ inch smooth circular pipes to

investigate the effect of inclination on liquid holdup and pressure loss in gas and liquid two-phase flow (Beggs and Brill, 1973). As a result of their experimental research, they produced the following correlation. Using this correlation, we calculated the pressure loss for our inclined and vertical section, depicted in our system diagram in figure 5a.

Calculate total flux rate

$$v_m = v_{sl} + v_{sg} \tag{10}$$

Calculate no-slip holdup

$$\lambda_{ns} = \frac{Vsl}{Vsl+Vsg} \tag{11}$$

Calculate the Froude number, NFR

$$N_{FR} = \frac{V_m 2}{gd} \tag{12}$$

Calculate liquid velocity number

$$N_{Lv} = V_{sl}\left(\frac{\rho l}{g\sigma_L}\right)^{0.25} \tag{13}$$

Calculate the correlating parameter, L_1, L_2, L_3 & L_4

$$L_1 = 316\lambda_{ns}^{0.302} \tag{14}$$

$$L_2 = 0.0009252\lambda_{ns}^{-2.4684} \tag{15}$$

$$L_3 = 0.10\lambda_{ns}^{-1.4516} \tag{16}$$

$$L_4 = 0.5\lambda_{ns}^{-6.738} \tag{17}$$

Determine the flow pattern using limits:

Segregated:

$$\lambda_{ns} < 0.01 \text{ and } N_{Fr} < L_1 \tag{18}$$

or

$$\lambda_{ns} \geq 0.01 \text{ and } N_{FR} < L_2 \tag{19}$$

Transition:

$$\lambda_{NS} \geq 0.01 \text{ and } L_2 < N_{FR} \leq L_3 \tag{20}$$

Intermittent:

$$0.01 \leq \lambda_{ns} < 0.4 \text{ and } L_3 < N_{Fr} \leq L_1 \tag{21}$$

or

Distributed:

$$\lambda_{ns} < 0.4 \text{ and } N_{FR} \geq L_1 \tag{22}$$

or

$$\lambda_{ns} \geq 0.4 \text{ and } N_{FR} > L_4 \quad (23)$$

Calculate the horizontal holdup λ_o

$$\lambda_o = \frac{a\lambda_{ns}^b}{N_{Fr}^c} \quad (24)$$

The values for a, b, and c are determined for each flow pattern from table 1. These empirical coefficients are plugged into the equation to calculate the horizontal holdup after the flow pattern has been determined. The value of *a* is multiplied by the no-slip hold up to the power of the *b* value. Froude's number is multiplied to the power of the *c* value (Maurer Engineering INC., 1994).

Calculate the inclination correction factor coefficient

$$C = (1-\lambda_{ns})\ln\left(d\lambda_{ns}^e N N_{Lv}^f N_{FR}^g\right) \quad (25)$$

The values for *d, e, f,* and g are determined for each flow condition from table 2. The values are dependent on the flow regime and direction, with the distributed uphill having no correction factor so, C will be zero giving ψ a value of one. The flow patterns have the same value for *d, e, f,* and g in the downhill direction. An interpolation should be performed if the flow is in the transition pattern (Maurer Engineering INC., 1994).

Calculate the liquid holdup inclination correction factor

$$\psi = 1 + C[\sin(1.8\theta) - 0.333\sin^3(1.8\theta) \quad (26)$$

Where θ is the deviation from horizontal axis.

Calculate the liquid hold-up.

$$\lambda = \lambda_o \psi \quad (27)$$

Apply Palmer Correction factor:

$$\lambda = 0.918 * \lambda \quad \text{for uphill flow} \quad (28)$$

$$\lambda = 0.541 * \lambda \quad \text{for downhill flow} \quad (29)$$

When flow is in transition pattern, take the average as follows:

$$\lambda = a * \lambda_1 + (1-a)\lambda_2 : \; a = \frac{L_3 - N_{Fr}}{L_3 - L_2} \quad (30)$$

Where λ_1 the liquid hold-up calculated assuming the flow is segregated and λ_2 is the liquid holdup assuming the flow is intermittent.

Calculate frictional factor ratio

$$\frac{f_{tp}}{f_{ns}} = e^s \quad (31)$$

Where, $S = \frac{\ln(y)}{-0.0523 + 3.182\ln(y) - 0.8725[ln(y)]^2 + 0.01853[\ln(y)]^4}$ (32)

And $y = \frac{\lambda_{ns}}{\lambda^2}$ (33)

S becomes unbounded at a point in the interval 1 < y < 1.2; and for y in this interval, the function S is calculated from

$$S = \ln(2.2y - 1.2) \quad (34)$$

Calculate the frictional pressure gradient

$$(N_{Re})_{ns} = \rho_{ns} * v_m * de/\mu_{ns} \quad (35)$$

Use this no-slip Reynolds number to calculate no-slip friction factor, $f_{ns}{}'$, using Moody's diagram, then convert it into Fanny friction factor $f_{ns} = f_{ns}{}'/4$.

The two-phase friction factor will be

$$f_{tp} = f_{ns} * \frac{f_{tp}}{f_{ns}} \quad (36)$$

The frictional pressure gradient is

$$\left(\frac{dp}{dx}\right)_f = \frac{2f_{tp}\,\rho_{ns} * v_m^2}{d_e} \quad (37)$$

EXPERIMENTAL SETUP AND PROCEDURES

The experimental methods included the observation of flow regimes and the measuring of pressure differences. This was achieved by designing an undulating piping system that included horizontal, inclined, and vertical pipe orientations as commonly seen in the petroleum industry. An air compressor was used to create the effect of gas flowing through the pipe, while a water pump was used to circulate water throughout the system. As shown in figure 5, the open channel system consists of sections 1.5 – 3 ft. long, 1 inch, and 1.5 diameter pipes installed in series emptying into a water tank. The system also consists of six pressure transducers, each installed before and after each experimental section of horizontal, vertical, and inclined orientations. Pressure gauges were also installed at the beginning and end of the entire system to monitor the system's overall pressure losses. Figure 5b shows a flow meter was installed before the air inlet to measure the flowrate of water by itself. The same was done with a pressure gauge to measure the air pressure. To record data from the pressure transducers, a Data Acquisition was installed to the back of the system's board connected to a computer. The electrical circuit of the DATAQ and pressure transducers is shown in figure 6.

DATAQ Circuit

The circuit consists of six pressure transducers, each powered by the DATAQ logging instrument. The DATAQ logging instrument is powered by the computer's CPU utilizing a USB, which transfers information. The transducers take the pressure readings and return the information to the DATAQ logging instrument, which is used to collect data. After the pressure readings are collected, it is sent to the computer to be interpreted using WinDaq recording and playback software.

Pipes & Fittings (Elbows)

Straight 1 and 1 ½ inch clear wall Schedule 80 PVC pipes were used for the experimental system. The pipes are able to withstand up to 200 psi 72° F and a maximum of 140° F. The fittings used are 45° & 90°, 1 and 1 ½ inch Schedule 80 PVC elbows that are also able to withstand up to 200 psi and a maximum of 140° F. To connect the pipes and elbows PVC primer and cement were used.

Water Pump

As shown in figure 3b, the water pump used in this experiment is a three-phase pump. It is compatible with a variable frequency drive which allows control of the water flow rate. The variable frequency drive ranges from 0 – 60 Hz where 60 Hz is equivalent to about 9.5 GPM.

Air Compressor

The air compressor, which is also shown in figure 3b, is the C2002, 6-Gallon, Oil-Free, Pancake Compressor. This pancake style compressor is constructed this way for increased stability. The compressor

also features a water drain valve and tough rubber legs. The compressor has air delivery at 40 psi of 3.5 SCFM and at 90 psi 2.6 SCFM.

PROCEDURE

A series of steps were carried out for the experimental work to be successful. The procedure of the experimental work is as follows:

1. Fill the Water Tank to ~25 Gal.
2. Turn on the Water Pump.
3. Turn on the Air Compressor.
4. Observe the flow regime through the different sections of the system.
    a. First, observe & record flow regime through the horizontal Pipe.
    b. Second, observe & record the flow regime through the inclined Pipe.
    c. Third, observe & record the flow regime through the vertical Pipe.
    d. Last, observe the flow regime through the smaller diameter pipe compared to the normal diameter pipe and note any difference.
5. Vary the Flowrates of water and air pressure to observe the differences in the four sections.
6. Report the different pressures at the gauges and pressure transducers.
7. Control choke valve to quarter, half, and three-quarter closed and record the influence on the pressure at the transducers.

RESULTS/DISCUSSION

Chock Valve Positions Effect on System Pressure

Based on the system calculations pressure losses, it was expected that the experimental pressure losses using this apparatus would be minimal, which was proven by the experiments. The main reason for the minimal loss and the low pressure of less than 2 psi is due to the system being an open one with an outlet pressure of 0 psi. There were minor pressure losses between the different sections and elbows. However, we were able to increase the system pressure by small fractions by partially closing the choke valve at the outlet of the pipe circuit to quarter, half, and three-quarter closed. The reason for adjusting the choke valve was to increase our quantitative results by evaluating what effect the choke valve at the end of the pipe circuit has on system pressure at key points in the system. Figures 7 and 8 depict the pressure difference from transducer 1 through 6 (labeled in figure 5a) at different flow rates and air pressures for the four choke valve positions. These positions are open, quarter, half, and three-quarter closed. After prior tests and careful consideration, we chose flow rates of 4 and 8 GPM and air pressures from 10 to 120 psi. Our reason for this was primarily to maintain multiphase flow conditions in our system and not have a more dominant phase to the point of a single-phase flow. For example, at flow rates less than 4 GPM, we notice that the water struggled to get through our system, especially at air pressures above 100 psi. Comparatively, when the flow rate was above 8 GPM, the changes in air pressure below 100 psi had little effect on the system, as water was the dominant phase. As it relates specifically to our choice of air pressure, we experimented with air pressure from 10 psi through 180 psi. However, pressure differences were identical at 10 through 60 psi and 70 through 180 psi, and decided it was best to record up to 120 psi. In addition, we also saw a greater variety of flow regime changes during observational experiments at these flow rates.

Figure 7 shows a comparison of pressure differences between a constant air pressure of 10 psi and differing water flow rates at 4 and 8 GPM influenced by the choke valve at the system's outlet. As shown in figure 7a, the closing of the choke value in three increments, didn't have a major effect on system pressure recorded at the transducers until the value was three-quarter closed. Though the initial pressure recorded at the first transducer and pressure at the fourth transducer were higher than all other choke valve positions, the greatest difference was at transducer three at the beginning of our 3-foot vertical section where flow direction changes by 90º. In contrast with figure 7b, where the water flow rate is doubled, there were more significant pressure differences for each choke valve position. Transducer one recorded the same pressure for open, quarter, and half-closed choke valve positions while pressure is higher at transducer two for these positions. It is important to note that pressure is the same at transducer four for all choke positions, indicating a 90º change in flow direction had no influence of system pressure in our system at low pressure.

Figure 8 also compares pressure differences between a constant air pressure of 120 psi and differing water flow rates at 4 and 8 GPM influenced by a choke valve at the outlet of the system. As shown in figure 8a, the closing of the choke value in three increments, didn't have a major effect on system pressure recorded at the transducers until the value was three-quarter closed. However, this effect is considerably smaller at high air pressures when figure 8a is compared to figure 7a. The only effect closing the choke had on the recorded system pressure was at transducer one at three-quarter closed. The pressure remains the same for all positions at the different choke positions. Figure 8b of 120 psi at 8 GPM shows more variation of pressures for the different choke positions; however, they are minimal.

Effect of Air Pressure, Flow Rate & Pipe Orientation on Flow Regimes

Experimental results consist of observed flow regimes for vertical, horizontal and inclined sections of the system. Air pressure varied in increments of 10psi to a maximum of 120 psi while the flow of water was kept constant and recorded in GPM. Figures 7 to 9 show the different flow regimes observed throughout the experiments performed.

Figure 7a shows stratified flow in the horizontal section of the experimental system. The system experienced stratified flow at a low water flow rate of 4 GPM up to 80 psi air pressure. Figure 7b shows stratified wavy flow in the same horizontal section as figure 7 of the experimental system. The system experienced stratified wavy flow at a water flow rates above 4 GPM for air pressures under 90 psi and for flow rates 6, 8 and 9 GPM for air pressure 10 – 120 psi.

Figure 8a shows bubble flow in the vertical section of the experimental system. The system experienced this flow regime at a high-water flow rate of 9 GPM and low for air pressures under 40 psi. Figure 8 b shows churn flow in the same vertical section as figure 8a and 8c of the experimental system. This flow regime occurred at high experimented water flow rates and air pressures. Figure 8c shows slug flow in the same vertical section as figure 8b of the experimental system. This flow regime occurred at each of the experimented water flow rates but became more prevalent at higher air pressures. Figure 9 shows plug flow in the 45º inclined section of the experimental system. This flow regime occurred at each of the experimented water flow rates with low air pressures below 70 psi.

The flow regimes observed in the system for the different flow rates of water and air was expected after previous theoretical calculation indicated turbulent flow using the Reynolds number from equation (3) and the Friction factor equation (4) then the Moody diagram. Stratified, Stratified Wavy, Bubble, Churn, Plug and Slug Flow were observed. More specifically, in the horizontal section Stratified Wavy Flow was observed throughout every variation of flow velocity and air pressure expect for 4 GPM water flow rates at air pressures less than 90 psi. In the vertical section the flow regimes varied between Slug, Churn and Bubble Flow and for the inclined section the flow regimes were predominately Plug and Slug Flow.

CONCLUSION

Using the Lockhart-Martinelli Parameter coupled with the Chisholm Equation and the Beggs & Brill Correlation method, we found that most of the hydrostatic pressure losses were in the elbows, and most frictional pressure loss occurred in the vertical 3ft pipe. In contrast, the 45° & 90° downhill pipes had an increase in pressure. Comparisons were made between the theoretical calculations and experimental results and in both instances, it was found that the majority of pressure loss occurred in the 45º and 90º elbows with the higher loss in the 90º compared to the 45º elbow. This proves that the higher the angle of inclination, the higher the pressure drop. The choke valve effect on system pressure was also determined by comparing four choke valve positions of open, ¼ closed. ½ closed, and ¾ closed at six key locations of the system where pressure transducers are located. These comparisons showed the closing of the choke value in increments had more effect on system pressure at lower air pressure and flow rates than during a high pressure and high flow rate environment. In addition, the partial closing of the choke valve had the most influence at the third transducer where it is positioned at the beginning of our vertical 3 ft. pipe where back pressure was expected to be highest. As it relates to flow regimes, the flow regimes observed were generally what was expected given prior calculations produced a Reynolds Number above 2300 for turbulent flow. Observed were churn flow, slug flow, plug flow, bubble flow, stratified and stratified wavy flow, as shown in tables 3 through 14. Specifically, in the horizontal section, stratified flow was observed at low air pressures and water flow rates and stratified wavy flow at higher flow rates and air pressures. In the

vertical section, the flow regimes varied between slug, bubble, and churn flow, and in the inclined section, the flow regimes also varied between slug and plug flow. Using the experimental system set up, we propose that future research can entail the effect of temperature on multiphase flow and the use of salt water or mineral oil.

NOMENCLATURE

f_{tp} = Two-phase friction factor

g = Gravitational acceleration (32.2 ft/ s2)

V_{sl} = Superficial liquid velocity (ft/s)

V_{sg} = Superficial gas velocity (ft/s)

V_m = Mixture velocity (ft/s)

Gpm = Gallons per Minute

psi = Pound per square inch

Ac= Cross-sectional area (m^2)

N_{Lv} = Calculate liquid velocity number

f_{H2O} = Friction factor water

f_{air} = Friction factor

f_{tp} = Two phase friction factor

$\left(\frac{dp}{dx}\right)_f$ =Frictional pressure gradient (psi)

j_{H2O} = Mass flux $(\frac{Kg}{sm^2})$

j_{air} = Find mass flux $(\frac{Kg}{sm^2})$

$\left(\frac{\Delta P}{L}\right)_{air}$ = Pressure gradient (Pa/m)

$\left(\frac{\Delta P}{L}\right)_{multi}$ = Pressure gradient (Pa/m)

$\left(\frac{\Delta P}{L}\right)_{H2O}$ = Pressure gradient $(Pa/m$

X = Lockhart-Martinelli parameter

d_e = Inner pipe diameter (mm)

Greek Symbols

λ_o = Horizontal holdup

λ = Palmer Correction factor

ψ = Liquid holdup inclination correction factor

φH_2O = Water pressure gradient multiplier

φ_{air} = Air pressure gradient multiplier

λ_{ns}= Calculate no-slip holdup

Dimensionless Group

N_{FR} = Froude number

R_{H2O}= Reynolds number (Pa/m)

R_{air} = Reynolds number, (Pa/m)

REFERENCES

Alagorni, A. H., Yaacob, Z. B., & Nour, A. H. (2015). An Overview of Oil Production Stages: Enhanced Oil Recovery Techniques and Nitrogen Injection. *International Journal of Environmental Science and Development*, *6*(9), 693–701. https://doi.org/10.7763/ijesd.2015.v6.682

Bai, Y., & Bai, Q. (2012). *Subsea Engineering Handbook* (1st ed.). Gulf Professional Publishing.

Baojiang, S. (2016). *Multiphase Flow in Oil and Gas Well Drilling* (First Edition). Higher Education Press.

Beggs, D. H., & Brill, J. P. (1973). A Study of Two-Phase Flow in Inclined Pipes. *Journal of Petroleum Technology*, *25*(05), 607–617. https://doi.org/10.2118/4007-pa

Chisholm, D. (1967). A theoretical basis for the Lockhart-Martinelli correlation for two-phase flow. *International Journal of Heat and Mass Transfer*, *10*(12), 1767–1778. https://doi.org/10.1016/0017-9310(67)90047-6

Corneliussen, S., Norwegian Society for Oil and Gas Measurement, & Tekna (Organization). (2005). *Handbook of Multiphase Flow Metering*. Norwegian Society for Oil and Gas Measurement.

Duns, H., & Ros, N. C. J. (1963). *Vertical flow of gas and liquid mixtures in wells*. In the 6th World Petroleum Congress, Frankfurt am Main, Germany.

Fancher, G. H., & Brown, K. E. (1963). Prediction of Pressure Gradients for Multiphase Flow in Tubing. *Society of Petroleum Engineers Journal*, *3*(01), 59–69. https://doi.org/10.2118/440-pa

Griffith, P. (1984). Multiphase Flow in Pipes. *Journal of Petroleum Technology*, *36*(03), 361–367. https://doi.org/10.2118/12895-pa

Hagedorn, A. R., & Brown, K. E. (1965). Experimental Study of Pressure Gradients Occurring During Continuous Two-Phase Flow in Small-Diameter Vertical Conduits. *Journal of Petroleum Technology*, *17*(04), 475–484. https://doi.org/10.2118/940-pa

Kleinstreuer, C. (2009). *Modern Fluid Dynamics*. Springer Publishing.

Kutty, S. S., & Babu, T. A. (2017). *Determination of Lockhart-Martinelli Parameter Using CFD in 2D Vertical Rectangular and offset Mini-Channels with R717*. International Journal of Applied Engineering Research.

Lockhart, R. W., & Martinelli, R. C. (1949). *Proposed Correlation of Data for Isothermal Two-Component Flow in Pipes*. Chem. Eng. Prog.

Maurer Engineering INC. *Multiphase Flow Production Model*. January 1994.

Michaelides, E., Crowe, C. T., & Schwarzkopf, J. D. (2016). *Multiphase Flow Handbook (Mechanical and Aerospace Engineering Series)* (2nd ed.). CRC Press.

Okoye, O. A. (2016). *Evaluation of Two-Phase Flow Characteristics In A Pipeline: Homogenous Model Approach* (No. 5). International Journal of Scientific & Technology Research.

Orkiszewski, J. (1967). Predicting Two-Phase Pressure Drops in Vertical Pipe. *Journal of Petroleum Technology*, *19*(06), 829–838. https://doi.org/10.2118/1546-pa

Sarah, A., Julius, U., & Mary-Ann, O. (2014). Pressure Gradient Prediction of Multiphase Flow in Pipes. *British Journal of Applied Science & Technology*, *4*(35), 4945–4958. https://doi.org/10.9734/bjast/2014/12985

Stuhmiller, J. H. (1977). The influence of interfacial pressure forces on the character of two-phase flow model equations. *International Journal of Multiphase Flow*, *3*(6), 551–560. https://doi.org/10.1016/0301-9322(77)90029-5

Taitel, Y., Bornea, D., & Dukler, A. E. (1980). Modelling flow pattern transitions for steady upward gas-liquid flow in vertical tubes. *AIChE Journal*, *26*(3), 345–354. https://doi.org/10.1002/aic.690260304

Zhang, D. Z., & Prosperetti, A. (1997). Momentum and energy equations for disperse two-phase flows and their closure for dilute suspensions. *International Journal of Multiphase Flow*, *23*(3), 425–453. https://doi.org/10.1016/s0301-9322(96)00080-8

Table 1: Flow Pattern Coefficient

Flow Pattern	a	b	c
Segregated	0.98	0.4846	0.0868
Intermittent	0.845	0.5351	0.0173
Distributed	1.065	0.5824	0.0609

Table 2: Correction Factor Coefficient

Flow Pattern	d	e	f	g
Segregated uphill	0.011	-3.768	3.539	-1.614
Intermittent uphill	2.96	0.305	-0.4473	0.0978
Distributed uphill	No Correction		C = 0	
All flow patterns downhill	4.70	-0.3692	0.1244	-0.5056

Table 3: 10 psi at 4,6,8, and 9 GPM

Air Pressure (psi)	Water Flowrate (GPM)	Direction	Pattern
10	4	Horizontal	Stratified Flow
		Incline	Plug Flow
		Vertical	Churn Flow
	6	Horizontal	Stratified Wavy Flow
		Incline	Plug Flow
		Vertical	Churn Flow
	8	Horizontal	Stratified Wavy Flow
		Incline	Plug Flow
		Vertical	Churn Flow
	9	Horizontal	Stratified Wavy Flow
		Incline	Plug Flow
		Vertical	Bubble Flow

Table 4: 20 psi at 4,6,8, and 9 GPM

Air Pressure (psi)	Water Flowrate (GPM)	Direction	Pattern
20	4	Horizontal	Stratified Flow
		Incline	Plug Flow
		Vertical	Slug Flow
	6	Horizontal	Stratified Wavy Flow
		Incline	Plug Flow
		Vertical	Churn Flow
	8	Horizontal	Stratified Wavy Flow
		Incline	Plug Flow
		Vertical	Churn Flow
	9	Horizontal	Stratified Flow
		Incline	Plug Flow
		Vertical	Bubble Flow

Table 5: 30 psi at 4,6,8, and 9 GPM

Air Pressure (psi)	Water Flowrate (GPM)	Direction	Pattern
30	4	Horizontal	Stratified Flow
		Incline	Plug Flow
		Vertical	Slug Flow
	6	Horizontal	Stratified Wavy Flow
		Incline	Plug Flow
		Vertical	Churn Flow
	8	Horizontal	Stratified Wavy Flow
		Incline	Plug Flow
		Vertical	Slug Flow
	9	Horizontal	Stratified Wavy Flow
		Incline	Plug Flow
		Vertical	Bubble Flow

Table 6: 40 psi at 4,6,8, and 9 GPM

Air Pressure (psi)	Water Flowrate (GPM)	Direction	Pattern
40	4	Horizontal	Stratified Flow
		Incline	Plug Flow
		Vertical	Slug Flow
	6	Horizontal	Stratified Wavy Flow
		Incline	Plug Flow
		Vertical	Slug Flow
	8	Horizontal	Stratified Wavy Flow
		Incline	Plug Flow
		Vertical	Slug Flow
	9	Horizontal	Stratified Wavy Flow
		Incline	Plug Flow
		Vertical	Slug Flow

Table 7: 50 psi at 4,6,8, and 9 GPM

Air Pressure (psi)	Water Flowrate (GPM)	Direction	Pattern
50	4	Horizontal	Stratified Flow
		Incline	Slug Flow
		Vertical	Slug Flow
	6	Horizontal	Stratified Wavy Flow
		Incline	Slug Flow
		Vertical	Slug Flow
	8	Horizontal	Stratified Wavy Flow
		Incline	Plug Flow
		Vertical	Slug Flow
	9	Horizontal	Stratified Wavy Flow
		Incline	Plug Flow
		Vertical	Slug Flow

Table 8: 60 psi at 4,6,8, and 9 GPM

Air Pressure (psi)	Water Flowrate (GPM)	Direction	Pattern
60	4	Horizontal	Stratified Flow
		Incline	Slug Flow
		Vertical	Slug Flow
	6	Horizontal	Stratified Wavy Flow
		Incline	Slug Flow
		Vertical	Slug Flow
	8	Horizontal	Stratified Wavy Flow
		Incline	Plug Flow
		Vertical	Slug Flow
	9	Horizontal	Stratified Wavy Flow
		Incline	Slug Flow
		Vertical	Slug Flow

Table 9: 70 psi at 4,6,8, and 9 GPM

Air Pressure (psi)	Water Flowrate (GPM)	Direction	Pattern
70	4	Horizontal	Stratified Flow
		Incline	Slug Flow
		Vertical	Slug Flow
	6	Horizontal	Stratified Wavy Flow
		Incline	Slug Flow
		Vertical	Slug Flow
	8	Horizontal	Stratified Wavy Flow
		Incline	Plug Flow
		Vertical	Slug Flow
	9	Horizontal	Stratified Wavy Flow
		Incline	Slug Flow
		Vertical	Slug Flow

Table 10: 80 psi at 4,6,8, and 9 GPM

Air Pressure (psi)	Water Flowrate (GPM)	Direction	Pattern
80	4	Horizontal	Stratified Flow
		Incline	Slug Flow
		Vertical	Slug Flow
	6	Horizontal	Stratified Wavy Flow
		Incline	Slug Flow
		Vertical	Slug Flow
	8	Horizontal	Stratified Wavy Flow
		Incline	Plug Flow
		Vertical	Slug Flow
	9	Horizontal	Stratified Wavy Flow
		Incline	Slug Flow
		Vertical	Churn Flow

Table 11: 90 psi at 4,6,8, and 9 GPM

Air Pressure (psi)	Water Flowrate (GPM)	Direction	Pattern
90	4	Horizontal	Stratified Wavy Flow
		Incline	Slug Flow
		Vertical	Slug Flow
	6	Horizontal	Stratified Wavy Flow
		Incline	Slug Flow
		Vertical	Slug Flow
	8	Horizontal	Stratified Wavy Flow
		Incline	Plug Flow
		Vertical	Slug Flow
	9	Horizontal	Stratified Wavy Flow
		Incline	Slug Flow
		Vertical	Churn Flow

Table 11: 90 psi at 4,6,8, and 9 GPM

Air Pressure (psi)	Water Flowrate (GPM)	Direction	Pattern
90	4	Horizontal	Stratified Wavy Flow
		Incline	Slug Flow
		Vertical	Slug Flow
	6	Horizontal	Stratified Wavy Flow
		Incline	Slug Flow
		Vertical	Slug Flow
	8	Horizontal	Stratified Wavy Flow
		Incline	Plug Flow
		Vertical	Slug Flow
	9	Horizontal	Stratified Wavy Flow
		Incline	Slug Flow
		Vertical	Churn Flow

Table 12: 100 psi at 4,6,8, and 9 GPM

Air Pressure (psi)	Water Flowrate (GPM)	Direction	Pattern
100	4	Horizontal	Stratified Wavy Flow
		Incline	Slug Flow
		Vertical	Slug Flow
	6	Horizontal	Stratified Wavy Flow
		Incline	Slug Flow
		Vertical	Slug Flow
	8	Horizontal	Stratified Wavy Flow
		Incline	Plug Flow
		Vertical	Slug Flow
	9	Horizontal	Stratified Wavy Flow
		Incline	Slug Flow
		Vertical	Churn Flow

Table 13: 110 psi at 4,6,8, and 9 GPM

Air Pressure (psi)	Water Flowrate (GPM)	Direction	Pattern
110	4	Horizontal	Stratified Wavy Flow
		Incline	Slug Flow
		Vertical	Slug Flow
	6	Horizontal	Stratified Wavy Flow
		Incline	Slug Flow
		Vertical	Slug Flow
	8	Horizontal	Stratified Wavy Flow
		Incline	Plug Flow
		Vertical	Slug Flow
	9	Horizontal	Stratified Wavy Flow
		Incline	Slug Flow
		Vertical	Churn Flow

Table 14: 120 psi at 4,6,8, and 9 GPM

Air Pressure (psi)	Water Flowrate (GPM)	Direction	Pattern
120	4	Horizontal	Stratified Wavy Flow
		Incline	Slug Flow
		Vertical	Slug Flow
	6	Horizontal	Stratified Wavy Flow
		Incline	Slug Flow
		Vertical	Slug Flow
	8	Horizontal	Stratified Wavy Flow
		Incline	Plug Flow
		Vertical	Slug Flow
	9	Horizontal	Stratified Wavy Flow
		Incline	Slug Flow
		Vertical	Churn Flow

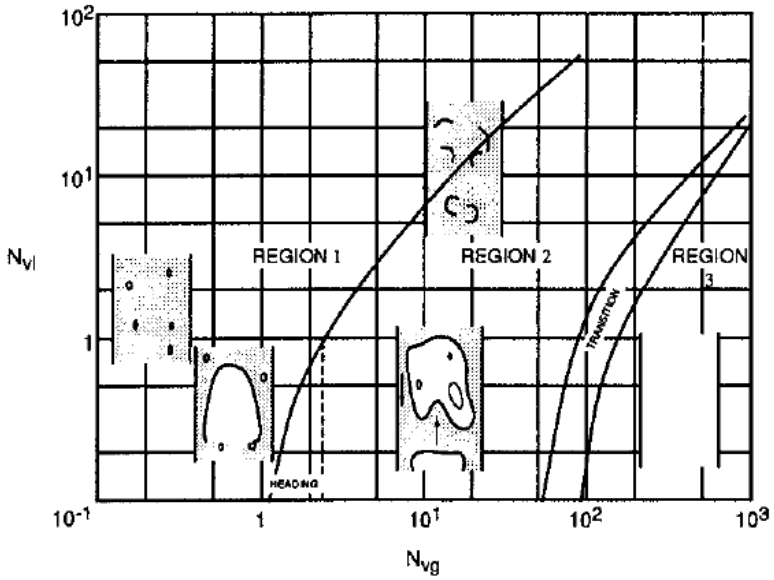

Figure 1: Duns and Ros Flow Regime Map (Duns and Ross, 1963)

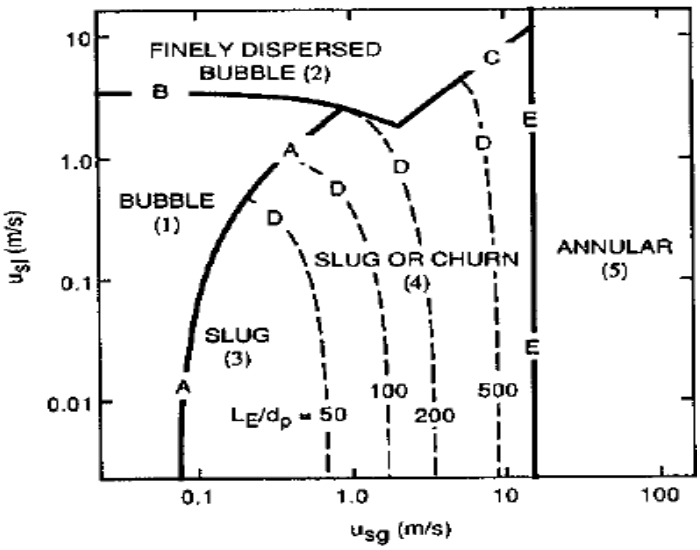

Figure 2: Taitel and Dukler Flow Regime Map (Taitel et al., 1980)

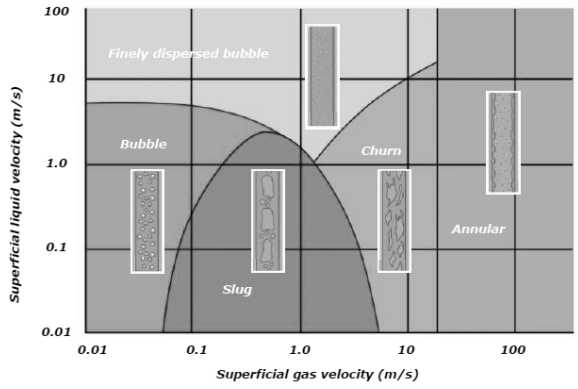

(a)

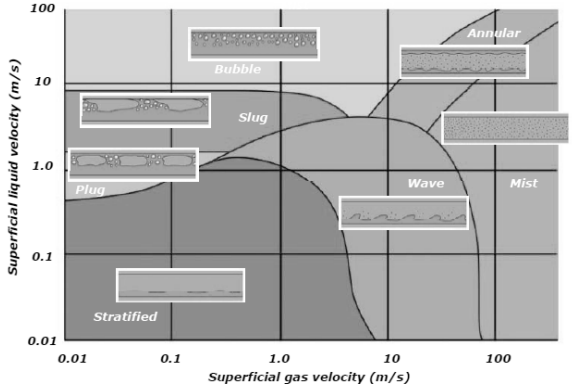

(b)

Figure 3: Flow Regime Maps **a)** Vertical Pipes **b)** Horizontal Pipes (Corneliussen et al., 2005)

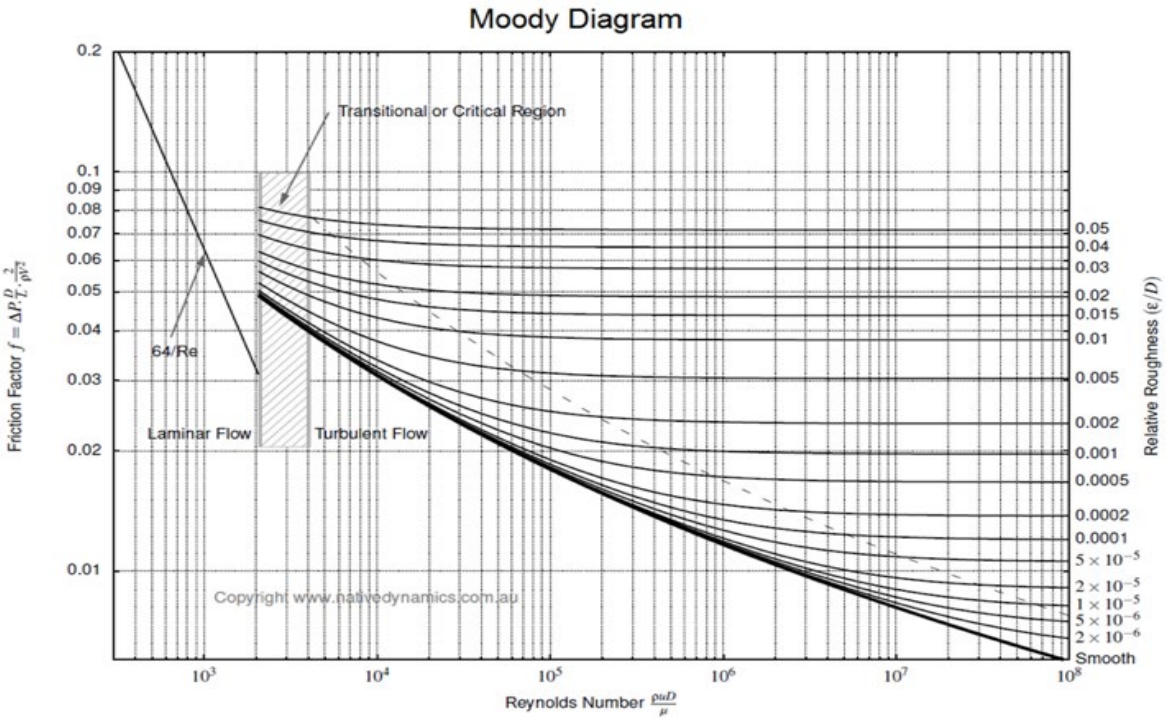

Figure 4: Moody Diagram: (Kleinstreuer C. Modern Fluid Dynamics. Springer, 2010)

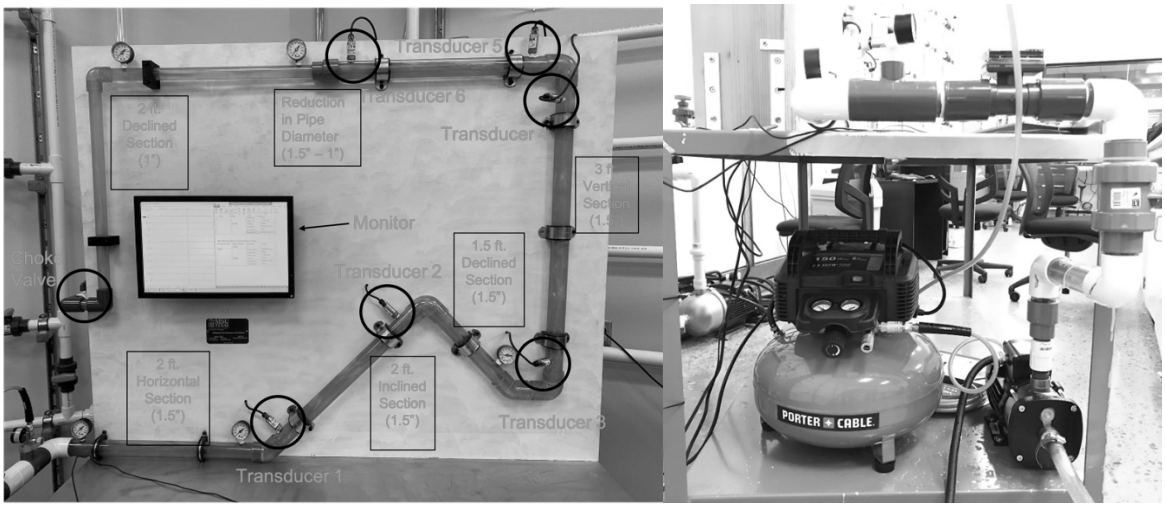

(a) (b)

Figure 5: Experimental System **a)** Piping System **b)** Air Compressor & Water Pump

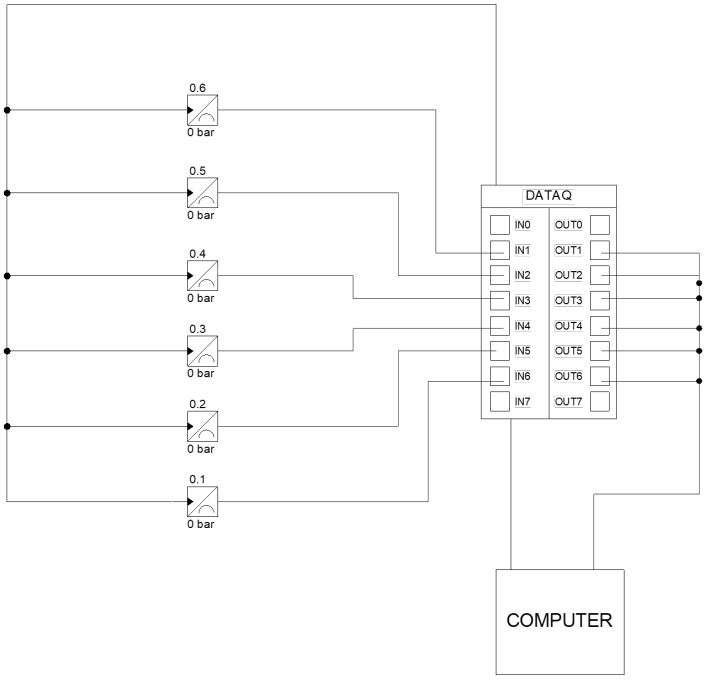

Figure 6: DATAQ and Pressure Transducer Circuit

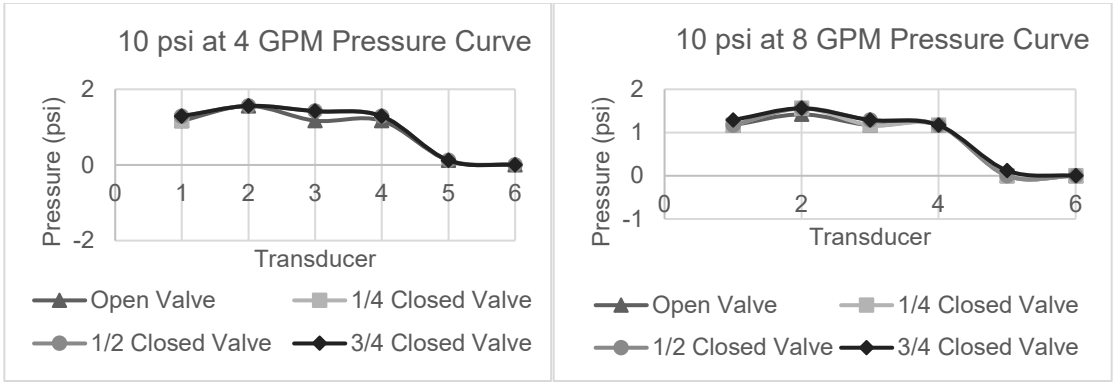

Figure 7: Pressure Curve a) 10 psi Air-Pressure at 4 GPM b) 10 psi Air-Pressure at 8 GPM

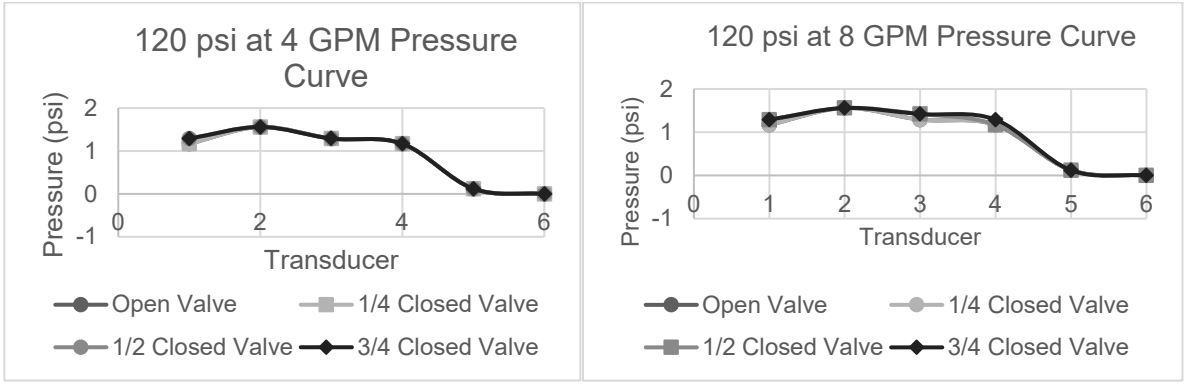

Figure 8: Pressure Curve a) 120 psi Air-Pressure at 4 GPM b) 120 psi Air-Pressure at 8 GPM

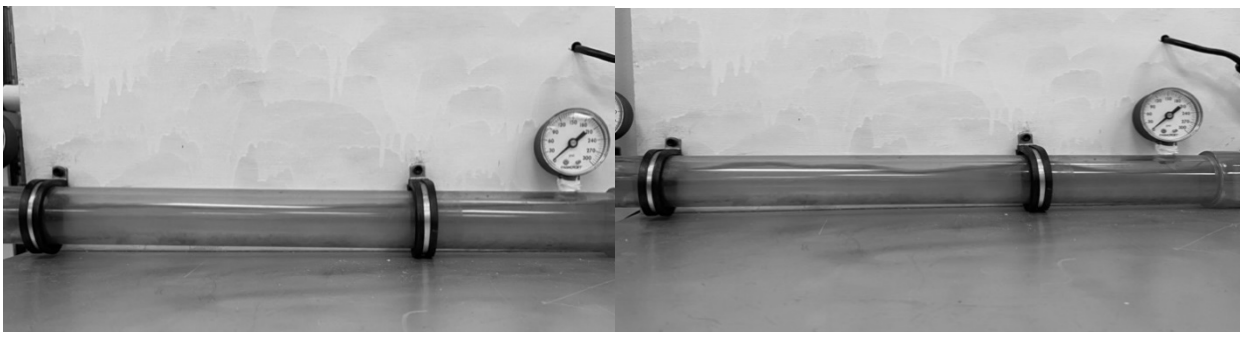

(a) (b)

Figure 9: Horizontal Section **a)** Stratified Flow **b**) Stratified Wavy Flow

Figure 10: Vertical Section a) Bubble Flow b) Churn Flow c) Slug Flow

Figure 11: Plug Flow in 45º Inclined Section